

Unsupervised Discretization by Two-dimensional MDL-based Histogram

Lincen Yang · Mitra Baratchi · Matthijs van Leeuwen

Received: date / Accepted: date

Abstract Unsupervised discretization is a crucial step in many knowledge discovery tasks. The state-of-the-art method for one-dimensional data infers locally adaptive histograms using the *minimum description length* (MDL) principle, but the multi-dimensional case is far less studied: current methods consider the dimensions one at a time (if not independently), which result in discretizations based on rectangular cells of adaptive size. Unfortunately, this approach is unable to adequately characterize dependencies among dimensions and/or results in discretizations consisting of more cells (or bins) than is desirable.

To address this problem, we propose an expressive model class that allows for far more flexible partitions of two-dimensional data. We extend the state of the art for the one-dimensional case to obtain a *model selection* problem based on the normalised maximum likelihood, a form of refined MDL. As the flexibility of our model class comes at the cost of a vast search space, we introduce a heuristic algorithm, named PALM, which partitions each dimension alternately and then merges neighbouring regions, all using the MDL principle. Experiments on synthetic data show that PALM 1) accurately reveals ground truth partitions that are within the model class (i.e., the search space), given a large enough sample size; 2) approximates well a wide range of partitions outside the model class; 3) converges, in contrast to its closest competitor IPD; and 4) is self-adaptive with regard to both sample size and local density structure of the data despite being parameter-free. Finally, we apply our algorithm to two geographic datasets to demonstrate its real-world potential.

Lincen Yang ✉
Leiden Institute of Advanced Computer Science, Leiden University
E-mail: l.yang@liacs.leidenuniv.nl

Mitra Baratchi
Leiden Institute of Advanced Computer Science, Leiden University
E-mail: m.baratchi@liacs.leidenuniv.nl

Matthijs van Leeuwen
Leiden Institute of Advanced Computer Science, Leiden University
E-mail: m.van.leeuwen@liacs.leidenuniv.nl

1 Introduction

Discretization, i.e., the transformation of continuous variables into discrete ones, is a task that is part of numerous data analysis workflows in practice. Although it can be used for many different purposes, it is mostly used for two main reasons.

The first reason is that many data mining and machine learning methods can deal with either continuous or discrete data as input, but not with both—one practical solution is to discretize continuous data. For example, pattern mining (Han et al., 2007; Vreeken et al., 2011) requires discrete data, naïve Bayes (Friedman et al., 2001) requires discrete data if one does not want to assume any parametric form (e.g., Gaussian) on the probability of the data, and classification and regression trees (Breiman, 2017) implicitly discretize continuous data. The second reason for using discretization is exploratory data analysis, i.e., getting to understand the data at hand, which should be the first phase of any data-driven project. Discretization can be very useful to this end, as histograms have the power to quickly provide the analyst an overview of the distribution of a continuous variable.

Although discretization is clearly a crucial step for a wide variety of applications in knowledge discovery and predictive modelling, many different methods exist and it is often not easy to determine which method should be used. As a result, naïve methods such as equal-length and equal-frequency binning are still widely used, often with the number of bins chosen more or less arbitrarily. This can lead to suboptimal results though, as information may get lost. Especially *unsupervised discretization*, i.e., discretization where no additional information on the goal of the analysis is available, is a hard problem, as it by definition leads to information loss when there are fewer bins than data points.

A good discretization strikes a balance between the amount of preserved information on one hand, and the complexity of the representation of the discretized data on the other hand. This balance is important to avoid discretizations that are either too coarse—resulting in too much information loss—or too fine-grained—in the extreme case resulting in a bin per data point. Achieving such balance is also the goal of locally adaptive histograms, of which the bins may have different widths and densities. Based on this idea, Kontkanen and Myllymäki (2007b) formalized the problem of selecting the best of such *variable-bin-size histograms* for a given set of data points using the *minimum description length* (MDL) principle.

The minimum description length (MDL) principle (Rissanen, 1978; Grünwald, 2007; Grünwald and Roos, 2019) is arguably the best off-the-shelf approach for this kind of model selection task, as it provides a means to naturally trade-off goodness-of-fit with model complexity. It achieves this by defining the “best” probabilistic model for some given data as the model that results in the best *compression* of data and model together. The MDL principle has been successfully applied to the task of inferring one-dimensional variable-bin-size histograms (Kontkanen and Myllymäki, 2007b), as well as to many other model selection tasks in machine learning and data mining (e.g., Hansen and Yu, 2001; Jörnsten and Yu, 2003; Robnik-Šikonja and Kononenko, 1998; Vreeken et al., 2011).

Multi-dimensional discretization. The methods that we have mentioned so far, however, have traditionally only been defined for one-dimensional (or univariate) data. That is, given a set of n one-dimensional data points denoted $z^n \in \mathbb{R}^n$, the discretization task is to partition the interval $[\min z^n, \max z^n]$ into a set of consecu-

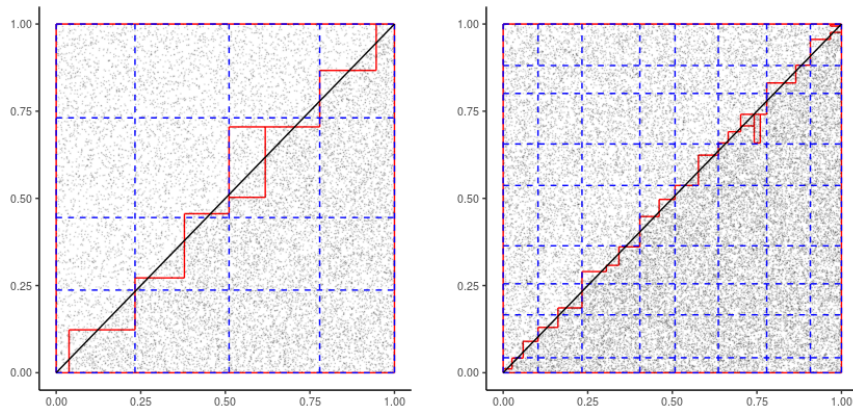


Fig. 1 Discretization of two-dimensional data with different densities in the upper-left and the lower-right triangles (black line). All data points are uniformly distributed. Left: 5 000 samples in upper-left triangle, 10 000 in bottom-right triangle. Right: ten times as many samples in each triangle. All data points are rounded to precision $\epsilon = 0.001$. Colored lines show discretization results obtained by 1) discretizing each dimension independently using one-dimensional MDL histograms (Kontkanen and Myllymäki, 2007b) (blue dashed); and 2) our algorithm (red solid).

tive subintervals and assign each data point to the subinterval to which it belongs. Whenever multi-dimensional (or multivariate) data needs to be discretized, the common approach in practice is to *discretize each dimension separately and independently*. This may result in suboptimal solutions though, as this approach ignores the dependencies that may exist between the dimensions.

To illustrate the limitations of independently discretizing individual dimensions, consider the toy example in Figure 1. In this example the sample space is $S = [0, 1] \times [0, 1] \subset \mathbb{R}^2$, and a line segment connecting points $(0, 0)$ and $(1, 1)$ partitions S into two triangles. The data points in each triangle are uniformly distributed, but with different densities. Within each plot, the upper triangle has twice as many data points as the lower triangle. Further, the right plot has ten times as many data points as the left one.

It is clear from Figure 1 that in this case it is impossible to find the optimal partition (or anything near it) by considering each dimension independently, simply because the two dimensions are strongly dependent. The blue dashed lines show the discretization result obtained by computing MDL-based histograms for each dimension independently, but the resulting partition has far more ‘bins’ than necessary. This brings us to the main question that we study in this paper: *how can we best perform multi-dimensional discretization, i.e., discretization that takes dependencies among dimensions into account?* One obvious problem of considering multiple dimensions at the same time is that the size of the search space can rapidly explode. Our key objective will therefore be to develop an algorithm that is not only flexible enough to consider a wide variety of partitions, but also computationally feasible, with a principled approach that does not require any hyper-parameters.

We restrict the scope of this paper to two-dimensional data and leave the extension to higher dimensional cases as future work. Focusing on two-dimensional cases allows us to clearly demonstrate the performance of our method by visualising

the discretization results. We will discuss the applicability to higher dimensional cases in Section 9.

Approach and contributions. The problem that we consider is an extension of the one-dimensional MDL-based histogram selection problem as introduced by Kontkanen and Myllymäki (2007b), i.e., we regard the task of inferring the best two-dimensional histogram as an MDL-based model selection task. We base our approach on this seminal work because it is both theoretically elegant and practically fast. Specifically, it adopts the *normalized maximum likelihood* (NML) encoding scheme that provides minimax regret, a form of *refined MDL*, and employs a fast dynamic programming algorithm to find the optimal solution.

Although an adaptive multivariate histogram usually refers to an adaptive grid, i.e., grid with locally variate “bin” size, the model class we consider is beyond that. In particular, given a fixed grid (i.e., grid with equal “bin” size) with a pre-determined granularity, we consider all possible clustering of “cells” of this fixed grid. This allows us to detect regions with flexible geometric shapes where data points are approximated uniformly distributed, as is shown in Figure 1. If desired, the granularity of this initial fixed grid can be set arbitrarily small, but in practice this is rarely needed as real-world data is typically recorded with a given precision.

Since efficiently finding the MDL-optimal two-dimensional histogram is infeasible, we next propose PALM, a novel heuristic algorithm that first partitions the data by iteratively partitioning each sub-region of the previous discretization result, and then iteratively merges neighbouring regions if their densities are similar enough; in all steps the MDL principle is used as decision criterion. As a result, our algorithm requires neither hyperparameters to be specified, nor any pre-defined stopping criterion. It is fully automatic and adapts to both local density structure (see Section 7.3) and sample size; the latter is shown in Figure 1, where the red solid lines show the partitions of the data as identified by our proposed method. Observe that the results closely approximate the ground truth, and that a larger sample size results in an even more accurate approximation.

Our contributions can be summarized as follows. First, we propose an MDL-based two-dimensional histogram model to tackle the unsupervised multivariate discretization task. Second, we improve the one-dimensional MDL-histogram algorithm both theoretically and practically. Third, we propose a search space for partitions together with a novel heuristic algorithm for the two-dimensional case, which combines top-down (partition) and bottom-up (merge) search strategies. Fourth, we empirically study the performance of our algorithm in the two-dimensional case, using both synthetic and real world data. The experiments show that our algorithm 1) can accurately recover ground truth histograms, 2) approximates well ground truth partitions that are not within the model class, and 3) outperforms IPD (Nguyen et al., 2014), the state-of-the-art multi-dimensional discretization algorithm.

The remainder of the article is organized as follows. We discuss related work in Section 2, formalise the problem as an MDL-based model selection task in Section 3, and describe the details of calculating the code length used in model selection in Section 4. We then briefly review the seminal algorithm used for inferring one-dimensional MDL-based histograms (Kontkanen and Myllymäki, 2007b), as well as how we improve it, in Section 5. We describe our algorithm, experiment

results and case study results based on the two-dimensional case in Sections 6, 7, and 8, and conclude in Section 9.

2 Related work

We briefly review previous work concerning discretization methods, tree-based models for density estimation, and similar techniques in other tasks.

Univariate discretization. Most unsupervised univariate discretization methods are rather straightforward, and are on equal-width binning, equal-frequency binning, or clustering techniques such as k-means (Friedman et al., 2001).

More advanced criteria rely on density estimation and specifically constructing variable-bin-width histograms. Apart from the MDL-based histogram (Kontkanen and Myllymäki, 2007b) already mentioned in Section 1, a variable-bin-size histogram can also be selected as the one whose density estimation result is closest to the result of *kernel density estimation* (Biba et al., 2007), where cross-validation is used to prevent overfitting. However, cross-validation is known to be computationally expensive, and the choice of kernel and bandwidth can be tricky in practice.

When discretization is needed for a supervised task such as classification, we can use *supervised discretization*, which means that the target variable is used to assess how much information on the target the discretization maintains. Several criteria can be put in this category, which are mostly based on statistical hypothesis testing or entropy, as summarized in the survey paper by Kotsiantis and Kanellopoulos (2006). The MDL principle has also been used for supervised discretization (Fayyad and Irani, 1993; Pfahringer, 1995; Zhang et al., 2007; Ferrandiz and Boullé, 2005; Gupta et al., 2010), but all of them use the so-called *crude MDL* principle (Grünwald, 2007).

Multivariate discretization. Since discretizing each dimension of multivariate data independently will ignore the dependencies among different dimensions, some methods attempt to reduce the dependencies by PCA- or ICA-based methods (Mehta et al., 2005; Kang et al., 2006). However, as both methods are based on *linear transformation* of the random vector, it is not possible for them to eliminate all kinds of dependencies.

Methods trying to optimize the discretization of all dimensions simultaneously also exist. One approach is to start from a very fine grid, and merge neighbouring subintervals for each dimensional if the multivariate probabilities of the data within these two consecutive subintervals are similar (Nguyen et al., 2014; Bay, 2001). These two methods are based on certain choices of similarity metrics, and require explicit specification of the similarity threshold.

Further, Kameya proposed to discretize two-dimensional data by iteratively adjusting the cut points on each dimension until convergence, using the coordinate descent optimization approach by applying the one-dimensional MDL-histogram iteratively (Kameya, 2011).

All these multivariate discretization methods, however, would fail on the toy example in Figure 1, and thus fail to characterize the dependencies present in such

cases. Further, we empirically show in Section 7 that IPD, the method by Nguyen et al. (2014) that is also based on the MDL principle, does not converge in practice.

Density estimation tree. Algorithmically, our method is very similar to methods using tree models for density estimation (Ram and Gray, 2011; Liu and Wong, 2014; Yang and Wong, 2014), as partitioning the data space by iteratively partitioning each dimension is the same as growing a tree. However, these density estimation trees were developed by adapting the scores used in growing, stopping, and pruning (supervised) decision and regression trees. That is, while our algorithm employs a consistent MDL-based framework for selecting the best model, these density estimation trees use separate optimisation scores respectively to fit the model and to control the model complexity, often with user-specified hyperparameters and/or computationally expensive cross-validation.

Moreover, these density estimation trees, as is like most supervised tree models, only do binary partitioning in a greedy manner. On the contrary, our method can split a dimension into multiple bins (from 1 to a pre-determined K_{max}) instead of just two, which is not only more flexible, but also more interpretable, as after partitioning on a certain dimension, within each bin the data points on that dimension can be regarded as approximately uniform.

Finally, our method consists of a merging step, which creates much more expressive partitions of data, and is hence more informative for pattern mining and exploratory data analysis.

Other tasks. Besides the discretization methods and histogram models, constructing a model by partitioning the data space is widely used in machine learning tasks. The MDL-based model selection framework has also been introduced in, e.g., image segmentation (Luo and Khoshgoftaar, 2006; Niblack and Steele, 1994), and object detection in computer vision (Leibe et al., 2008).

3 Problem Statement

Informally, we consider the problem of inferring the ‘best’ two-dimensional histogram for a given sample of continuous data. To make this problem precise, we start off by introducing our notation and definitions. Note that all $\log(\cdot)$ should be read as $\log_2(\cdot)$ unless specified otherwise.

3.1 Notation and definitions of data, model, and model class

Consider as data a vector of length n , i.e., $x^n = (x_1, \dots, x_n)$, sampled independently from the *random variable* X .

The *sample space* of X , denoted as S , is a *bounded* subset of \mathbb{R}^2 . Although the sample space of a random variable, e.g., a Gaussian, can be infinite in theory, we always assume it to be a bounded “box” when dealing with a given dataset. The task of estimating S from the data directly is another research topic, usually referred to as “support estimation” in statistical literature (Cuevas et al., 1997), and hence is out of the scope of our main focus in this article.

Conceptually, a histogram—no matter whether it is one- or multi-dimensional—is a *partition* of the sample space S , denoted by \tilde{S} and parametrized by a vector $\mathbf{f} = (f_1, \dots, f_K)$. A partition \tilde{S} is defined as a set of *disjoint* subsets (also referred to as sub-regions) of S , and the union of all these subsets is S itself, i.e., $\tilde{S} = \{S_1, S_2, \dots, S_K\}$, where $\forall j \in \{1, \dots, K\}$, $S_j \subseteq S$, $\bigcup_{j=1}^K S_j = S$, and $\forall j, k \in \{1, \dots, K\}$, $S_j \cap S_k = \emptyset$.

Next, we assume that the probability density of X , denoted by $f(X)$, is given by

$$f(X) = \sum_{j \in \{1, \dots, K\}} \mathbb{1}_{S_j}(X) f_j, \quad (1)$$

where $\mathbb{1}_{\{\cdot\}}(\cdot)$ is the *indicator function*. Each f_j is a *constant* and \mathbf{f} satisfies $\sum_{i=1}^K f_i |S_i| = 1$, where $|S_j|$ denotes the geometric area of S_j , i.e., when $X \in S_j$, $f(X) = f_j$. We refer to any partition \tilde{S} as a *histogram model* that contains a family of probability distributions; i.e., $\forall \mathbf{f} \in \mathbb{R}^K$, we denote a single probability distribution by $\tilde{S}_{\mathbf{f}}$.

We denote the model class as \mathbb{M} , representing all possible partitions that can be obtained by clustering cells of a fixed grid covering S , with granularity of ϵ . Geometrically, this is equivalent to drawing *inner boundaries* within S along the fixed grid. In practice, ϵ can represent the precision up to which the data is recorded or that is useful for the given task. Although the model class we consider can only produce inner boundaries like a “step function”, we will show that such model class is flexible enough to approximate curve inner boundaries in Section 7.

3.2 Histogram model selection by the MDL principle

We now formally define the task of two-dimensional data discretisation as a MDL-based model selection task, using histogram models as the model class.

The MDL principle is arguably the best off-the-shelf model selection method and has been successfully applied to many machine learning tasks (Grünwald, 2007; Hansen and Yu, 2001). It has solid theoretical foundations in information theory and naturally prevents overfitting as the optimization criterion always includes the model complexity, defined as the code length (in bits) needed to encode that model (Grünwald, 2007).

The basic idea is to *losslessly encode* the model and data together, by firstly encoding the model and then compressing the data using that model. Then the model resulting in the shortest total *code length* is defined to be MDL-optimal, i.e.,

$$\tilde{S}^* = \arg \min_{\tilde{S} \in \mathbb{M}} L(x^n, \tilde{S}) = \arg \min_{\tilde{S} \in \mathbb{M}} (L(\tilde{S}) + L(x^n | \tilde{S})), \quad (2)$$

where $L(\tilde{S})$ and $L(x^n | \tilde{S})$ are the code length of the model and the code length of the data compressed by that model, respectively. Generally, $L(\cdot | \cdot)$ represents the *conditional* code length (Grünwald, 2007); informally, $L(A | B)$ represents the code length of the message a *decoder* needs to receive in order to be able to losslessly reconstruct message A after having already received message B .

Unfortunately, we will show in Section 4 that properly encoding the model and calculating its corresponding code length $L(\tilde{S})$, and hence $L(x^n, \tilde{S})$ as defined by

Equation (2), turns out to be very difficult. As a result, we cannot regard our model selection task simply as an optimisation problem.

To alleviate this, we divide the model selection task into two steps, namely partitioning alternately and merging.

First, we alternately split each sub-region within the partition \tilde{S} (initially $\tilde{S} = \{S\}$) on one of the two dimensions, then update the partition \tilde{S} accordingly, and repeat the process. In other words, at each iteration with the partition \tilde{S} obtained so far, we further split each sub-region within \tilde{S} at a certain dimension (i.e., horizontally or vertically), which is equivalent to selecting the best set of horizontal or vertical *cut lines*. Denote the subset of data points within a certain sub-region $S' \in \tilde{S}$ as $\{x^n \in S'\}$, and we formally define the task of selecting the MDL-optimal cut lines set as

$$\begin{aligned} C_{S'}^* &= \arg \min_{C_{S'} \in \mathbb{C}_{S'}} L(\{x^n \in S'\}, C_{S'}) \\ &= \arg \min_{C_{S'} \in \mathbb{C}_{S'}} (L(C_{S'}) + L(\{x^n \in S'\} | C_{S'})), \end{aligned} \quad (3)$$

where $\mathbb{C}_{S'}$ are all possible sets of positions of cut lines, containing $K = \{0, 1, \dots, K_{max}\}$ cut lines, for one certain sub-region $S' \in \tilde{S}$, on one certain dimension (i.e., horizontal or vertical), and K_{max} is predetermined in priori to be “large enough” given the task at hand. In practice, post-analysis can be used to determine whether larger K_{max} should be investigated, by checking whether the likelihood of data is (almost) converged before the number of bins reaches $K_{\{max\}}$.

In Section 5, we will show that searching for the MDL-optimal cut lines for (a subset of) two-dimensional data is the same as searching for the MDL-optimal cut points for the one-dimensional data, which is the projection of two-dimensional data on x- or y-axis.

The partitioning step will automatically stop once for each sub-region the MDL-optimal set of cut lines is the null set, i.e., no further partitioning is needed.

Second, we search for all possible clustering of sub-regions gained in the previous alternately partitioning step, in a greedy manner. In other words, we constrain the model class \mathbb{M} which contains all possible clustering of cells of a fixed grid to be all possible clustering of sub-regions of the partition gained by the alternately partitioning step. We denoted this constrained model class by \mathbb{M}_c , and we formally define the merging step as selecting the MDL-optimal model within \mathbb{M}_c , i.e.,

$$\tilde{S}_{merge}^* = \arg \min_{\tilde{S} \in \mathbb{M}_c} L(x^n, \tilde{S}) = \arg \min_{\tilde{S} \in \mathbb{M}_c} (L(\tilde{S}) + L(x^n | \tilde{S})). \quad (4)$$

We will discuss the calculation of code length of data and model in Section 4, and then describe our algorithm in detail in Section 6, after revisiting the one-dimensional MDL histogram algorithm (Kontkanen and Myllymäki, 2007b), on which our algorithm is based, in Section 5.

4 Calculating the code length

In this section, we discuss the details of the code length (in bits) needed to encode the data and the model.

We first prove that the code length of the data given a histogram model, encoded by the normalized maximum likelihood (NML) code (Grünwald, 2007; Grünwald and Roos, 2019), is independent of its dimensionality. As a result, given any partition \tilde{S} of a two-dimensional sample space S , the code length of two-dimensional data $L(x^n|\tilde{S})$ can be calculated almost in the same way as one-dimensional data. Although the proof itself turns out to be trivial, the outcome is surprisingly useful.

We then discuss in detail the difficulties of encoding all possible models $\tilde{S} \in \mathbb{M}$ if we would want to directly optimise over the full model class \mathbb{M} using Equation (2). We show that encoding all possible models may result in substantial code length redundancy, or involve challenging combinatorial counting, which motivates our (somewhat ad-hoc) solution of dividing the model selection task in two separate steps.

Finally, we discuss the calculation of the code length of a model in the partitioning and merging step respectively, i.e., $L(C_{S'})$ and $L(\tilde{S})$ of Equations (3) and (4).

4.1 Code length of the data

Extending the work that was previously done for the one-dimensional case (Konkkanen and Myllymäki, 2007b), we use the same code—i.e., the *Normalized Maximum Likelihood* (NML) code—to encode the two-dimensional data. This code has the desirable property that it is theoretically optimal because it has minimax regret. The code length of the NML code is given by

$$L(x^n|\tilde{S}) = -\log \left[\frac{P(x^n|\tilde{S}_{\hat{\mathbf{f}}(x^n)})}{\text{COMP}(n, \tilde{S})} \right], \quad (5)$$

where $P(x^n|\tilde{S}_{\hat{\mathbf{f}}(x^n)})$ is the probability of the data given $\tilde{S}_{\hat{\mathbf{f}}(x^n)}$, i.e., the parameters $\mathbf{f} = (f_1, \dots, f_K)$ are estimated by the *maximum likelihood estimator* given dataset x^n , denoted as $\hat{\mathbf{f}}(x^n) = (\hat{f}_1, \dots, \hat{f}_K)$. The term $\text{COMP}(n, \tilde{S})$ is the so-called *parametric complexity*, which is defined as

$$\text{COMP}(n, \tilde{S}) = \sum_{y^n \in S^n} P(y^n|\tilde{S}_{\hat{\mathbf{f}}(y^n)}), \quad (6)$$

where $\sum_{y^n \in S^n}$ is the sum over *all possible sequences* y^n within the Cartesian product of sample space S that can be *generated* by the histogram model \tilde{S} , i.e., the order of y^n *does* matter.

We will now first describe the calculation of $P(x^n|\tilde{S}_{\hat{\mathbf{f}}(x^n)})$, and then the calculation of $\text{COMP}(n, \tilde{S})$.

For any single data point $x_i \in x^n$, let $x_i = (x_{i1}, x_{i2})$ denote the pair of values for its two dimensions.

$$P(x^n|\tilde{S}_{\hat{\mathbf{f}}(x^n)}) = \prod_{i=1}^n P(x_i|\tilde{S}_{\hat{\mathbf{f}}(x^n)}) = \prod_{j=1}^K \left(\prod_{x_i \in S_j} P(x_i|\tilde{S}_{\hat{\mathbf{f}}(x^n)}) \right) \quad (7)$$

as the data points are assumed to be independent. Note that K represents the number of sub-regions of \tilde{S} .

Since we assume our data to have precision ϵ , we can define the probability of the data as (also referred to as its *maximum likelihood*):

$$P(x_i | \tilde{S}_{\hat{f}(x^n)}) = P(X \in [x_{i1} - \frac{\epsilon}{2}, x_{i1} + \frac{\epsilon}{2}] \times [x_{i2} - \frac{\epsilon}{2}, x_{i2} + \frac{\epsilon}{2}] | \tilde{S}_{\hat{f}(x^n)}) = \hat{f}_j \epsilon^2. \quad (8)$$

The maximum likelihood estimator for the histogram model (Scott, 2015) is

$$\hat{f}_j = \frac{h_j}{n |S_j|}, \forall j, \quad (9)$$

where h_j is the number of data points within S_j , and $|S_j|$ is the area of S_j . Thus, following Equations (7),(8), and (9),

$$P(x^n | \tilde{S}_{\hat{f}(x^n)}) = \prod_{j=1}^K (\hat{f}_j \epsilon^2)^{h_j} = \prod_{j=1}^K \left(\frac{h_j \epsilon^2}{n |S_j|} \right)^{h_j}. \quad (10)$$

Now we describe the calculation of $\text{COMP}(n, \tilde{S})$. Kontkanen and Myllymäki (2007b) proved that, for one-dimensional histograms, $\text{COMP}(n, \tilde{S})$ is a function of only sample size n and the number of bins K , and thus can be denoted as $\text{COMP}(n, K)$. Following the same mathematical analysis, we (trivially) prove that for the multi-dimensional case, $\text{COMP}(n, \tilde{S})$ is the same as for the one-dimensional case, i.e., it is independent of the dimension of S (see the proof in Appendix A). Specifically,

$$\text{COMP}(n, K) = \sum_{h_1 + \dots + h_K = n} \frac{n!}{h_1! \dots h_K!} \prod_{j=1}^K \left(\frac{h_j}{n} \right)^{h_j}, \quad (11)$$

which turns out to be the same as the parametric complexity for the multinomial model (Kontkanen and Myllymäki, 2007a). It has also been proven that we can calculate $\text{COMP}(n, K)$ in linear time (Kontkanen and Myllymäki, 2007a) by means of the following recursive formula:

$$\text{COMP}(n, K) = \text{COMP}(n, K - 1) + \frac{n}{K - 2} \text{COMP}(n, K - 2). \quad (12)$$

Apart from the fact that the parametric complexity is independent of the number of dimensions, the probability of the data is also almost the same for different dimensionalities. The only difference lies in the exponent given to ϵ , i.e., the term ϵ^2 in Equation (10) becomes ϵ^l for an l -dimensional histogram, which is a constant and hence can be ignored for model selection (assuming we fix the dimensionality). This is not surprising after observing that the mathematical form of the probability of the data is determined by the ‘‘counts’’ of the data within each sub-region, regardless of dimensionality.

4.2 Code length of the model

We will first discuss in detail why properly encoding all models in the model class is difficult, and will then describe the code length of model in the partitioning step and the merging step.

4.2.1 Encoding all models in the model class is difficult

Generally, there are two ways of encoding a model: one is to encode the model explicitly, the other is to encode the model from a Bayesian perspective, using the so-called *index code*. In the following, however, we will show that neither approach is directly applicable if we were to encode all histogram models $\tilde{S} \in \mathbb{M}$ and directly optimise Equation (2): explicitly encoding the model would cause substantial code length redundancy, meaning that we would significantly overestimate the model complexity; meanwhile, using the index code would involve very complicated combinatorial counting.

Explicitly encoding the model. An intuitive way of encoding the histogram model is to explicitly encode its geometric shape. Given a dataset with a “bounding box” as its *support*, we could encode all the inner boundaries by encoding the positions of the line segments that constitute the set of inner boundaries. This encoding scheme may cause substantial code length redundancy though, as an arbitrary set of line segments is unlikely to form a valid partition of S and even a valid partition would be likely to have superfluous, useless line segments.

Another common approach for explicit encoding is to index each cell of the grid which our model class is based on, and encode which cells belong to which cluster, by assigning the label of a cluster to each cell and encoding a sequence of cluster labels. This approach is also redundant since an arbitrary sequence of cluster labels does not necessarily represent a valid partition of data.

A Bayesian perspective and the index code. From a Bayesian perspective, regardless of how we encode all candidate models, we would always specify a prior distribution on the model class, because models with shorter code lengths are more likely to be selected a priori than those with longer code lengths (as we would search for the model that minimizes $L(x^n|\tilde{S}) + L(\tilde{S})$).

In practice, sometimes it is useful to have the explicit control on the prior distribution, instead of explicit control of the encoding process. This can be achieved by using the so-called *index code*: we first index all possible models $\tilde{S} \in \mathbb{M}$, and then simply encode the index of each model. In this way, we are actually assigning different code lengths to each model rather than “encoding” the model explicitly. As long as a corresponding code with such code lengths exists, we can assume that the encoding is done implicitly. We only need the code length for the model selection task after all. In fact, the theory of *Kraft inequality* guarantees that as long as we specify a proper prior distribution (i.e., sum of probabilities of all models smaller or equal to 1) on the models, a corresponding code for each model with code length equal to the logarithm of prior probability of that model always exists (Grünwald, 2007). It also guarantees that the corresponding code has no code length redundancy if and only if the sum of probabilities equal to 1, which is an advantage of using index code over explicitly encoding the model.

Index code is particularly useful when there are some hierarchical structures within the model class \mathbb{M} that characterise the model complexity. A common practice in the MDL-based model selection tasks is to divide the model class into disjoint subsets of models according to the hierarchical structures of model complexity, and assign a uniform prior to each model within each subset of the model class. As in our case, the only obvious ways (to us) of dividing the model

class into subsets are according to their number of sub-regions, the number of line segments in the inner boundary set, or the combination of them, and treat the histogram models within each subset of model class to have the same complexity (and hence assign a uniform prior to them).

However, this approach turns out to be not directly applicable for our task either: to calculate the code length of uniform code (i.e., the probability of discrete uniform distribution), we need to count the number of models within each subset of model class, which turns out to be very challenging for our task. The fact that our full model class \mathbb{M} is based on a grid makes it a difficult combinatorial problem to count the number of models in each subset of models, if we divide the model class based on the number of sub-regions of the histogram model, and/or based on the number of line segments of the inner boundary.

4.2.2 Code length of the model in the partitioning and merging steps

As properly encoding all possible models within \mathbb{M} turns out to be too difficult, we now discuss how to calculate the code length of model in the partitioning and merging step respectively. We stick to the index code to avoid code length redundancy.

Partitioning. For a sub-region $S' \in \tilde{S}$, assume that there are E candidate positions for cut lines, horizontal or vertical. To encode the set of cut lines, we first encode the number of sub-regions $K \in \{1, \dots, K_{max}\}$, where K_{max} is predetermined. We assign a uniform prior on K , and thus the code length needed to encode K becomes a constant, which has no effect on the result of the partitioning step. Given K , we then encode the positions of $(K - 1)$ cut lines, with again a uniform prior on all possible sets of $(K - 1)$ cut lines. The code length needed in bits is

$$L(C_{S'}) = \log \binom{E}{K-1} \quad (13)$$

Merging. When the partitioning step has stopped, the constrained model class \mathbb{M}_c for the merging step is also fixed, which contains all possible models that can be obtained by merging neighbouring sub-regions of the partition after the partitioning step. To encode all models within \mathbb{M}_c , we use the index code and assign a uniform prior to all of them.

The merging step tends to add geometric complexity to the histogram model on one hand, but will reduce the number of parameters on the other hand. Therefore, we treat them with equal model complexity a priori. As a result, the code length of all models within \mathbb{M}_c is a constant and has no effect on the result of the merging step. In other words, we only consider the code length of data in the merging step.

5 Revisiting MDL histograms for one-dimensional data

We first show that searching for the best cut lines on one certain dimension of given two-dimensional data is equivalent to searching for the best cut points for the corresponding one-dimensional data. We then review the algorithm for inferring MDL histograms for one-dimensional data as proposed by Kontkanen and

Myllymäki (2007b), and describe how we improve it both theoretically and practically.

Notation and relation to our problem. To be able to distinguish it from two-dimensional data x^n , we denote one-dimensional data as $z^n = (z_1, \dots, z_n)$, with precision equal to ϵ . Further, we define the sample space of z^n as $S^1 = [\min z^n, \max z^n]$.

We define the one-dimensional histogram model with K bins as a set of *cut points*, denoted as $C^K = \{C_0 = \min z^n, C_1, \dots, C_K = \max z^n\} \subseteq C_a$, with $K \in \{0, 1, \dots, K_{max}\}$, where K_{max} is pre-determined and C_a is defined as

$$C_a = \{\min z^n, \min z^n + \epsilon, \dots, \min z^n + E \cdot \epsilon, \max z^n\}, \quad (14)$$

with $E = \lfloor \frac{\max z^n - \min z^n}{\epsilon} \rfloor$. Note that we assume all subintervals to be closed on the left and open on the right, except that the rightmost subinterval is closed on both sides.

The code length needed to encode the model C^K is $L(C^K) = \log \binom{E}{K-1}$ by the index code, which is the same as Equation (13). Further, as is discussed in Section 4.1, the probability of one-dimensional data given such a model differs by a constant for that of two-dimensional data, and the parametric complexity is independent of the number of dimensions; therefore, the code length needed to encode z^n given C^K by the NML code is

$$\begin{aligned} L(z^n|C^K) &= -\log P(z^n|C^K) + \log \text{COMP}(n, K) \\ &= -\log \prod_{j=1}^K \left(\frac{h_j \epsilon}{n(C_{j+1} - C_j)} \right)^{h_j} + \log \text{COMP}(n, K). \end{aligned} \quad (15)$$

If we compare $L(z^n|C^K)$ and $L(C^K)$ with Equations (10) and (13), we can see that the definition of the two-dimensional MDL-optimal cut lines and the one-dimensional MDL-optimal cut points only differ by a constant. Thus, given a two-dimensional dataset $x^n = \{(x_{11}, x_{21}), \dots, (x_{1n}, x_{2n})\}$, the optimisation task of searching for the MDL-optimal vertical (or horizontal) cut lines is equivalent to the task of searching for the MDL-optimal one-dimensional cut points based on one-dimensional dataset $z^n = \{x_{11}, \dots, x_{1n}\}$ (or $z^n = \{x_{21}, \dots, x_{2n}\}$). That is, z^n is the projection of x^n on the x- or y-axis.

In other words, the algorithm for constructing MDL-based one-dimensional histogram proposed by Kontkanen and Myllymäki (2007b) can be directly applied to the partitioning step of our model selection task. We now briefly review this algorithm and show how we improve it both theoretically and practically.

Contributions. We improve the one-dimensional algorithm proposed by Kontkanen and Myllymäki (2007b) in two ways. First, in the previous work, the candidate cut points, denoted as C'_a , are chosen based on the data z^n , i.e., $C'_a = \bigcup_{i=1}^n \{z_i \pm \epsilon\}$, and hence the code length of model is calculated dependent on given dataset, i.e., $L(C^K|z^n)$ is calculated instead of $L(C^K)$, which is theoretically sub-optimal, because generally

$$L(z^n, C^K) = L(z^n|C^K) + L(C^K) \neq L(z^n|C^K) + L(C^K|z^n). \quad (16)$$

In practice, this will cause significantly worse results when the sample size is very small. Under such cases, the size of the set C'_a will be very small, and hence

the code length of model will be significantly underestimated, leading to serious overfitting. We fix this problem by encoding the model independent of the data.

Further, we show that, we do not need to consider all candidate cut points within C_a , but just those cut points with a data point near it from left or right, without other cut points in between; this reduces the search space to a subset of C_a , and hence reduce the computational requirements. We include the proof in Appendix B.

Finally, we simplify the recursion formula for the dynamic programming proposed by Kontkanen and Myllymäki (2007b) in their original paper, which significantly reduces empirical computation time.

Dynamic programming algorithm. We now describe the dynamic programming algorithm for one-dimensional data, as well as how we improve its recursion formula.

Kontkanen and Myllymäki (2007b) derived the recursion formula based on the total code length $L(z^n, C^K)$, i.e.,

$$\begin{aligned} L(z^n, C^K) &= L(z^n|C^K) + L(C^K) \\ &= -\log(P(z^n|C^K)) + \log \text{COMP}(n, K) + \log \binom{E}{K-1}. \end{aligned} \quad (17)$$

We show that we can simplify the recursion by only including the probability of the data, i.e., $P(z^n|C^K)$, instead of $L(z^n, C^K)$. Observe that when the number of bins K is fixed, $L(C^K)$ and $\text{COMP}(n, K)$ become constant. Then, for fixed K , minimizing $L(z^n, C^K)$ is equivalent to minimizing $\{-\log(P(z^n|C^K))\}$, i.e., maximizing the likelihood.

Therefore, minimizing $L(z^n, C^K)$, for all $K \in \{1, \dots, K_{max}\}$, can be done in two steps: 1) find the maximum likelihood cut points with fixed K , denoted as \hat{C}^K , for each K , using the following dynamic algorithm; and 2) calculate $L(z^n|\hat{C}^K)$ for each K , and find the $\hat{K} \in \{1, \dots, K_{max}\}$ that minimizes $L(z^n, \hat{C}^{\hat{K}})$. Then,

$$\hat{C}^{\hat{K}} = \arg \min_{K \in \{1, \dots, K_{max}\}, C^K \in C_a} L(z^n, C^K). \quad (18)$$

Now we describe the dynamic programming algorithm for finding \hat{C}^K for each $K \in \{1, \dots, K_{max}\}$. The (log) probability of z^n given any cut points is

$$\begin{aligned} \log P(z^n|C^K) &= \sum_{i=1}^n \log P(z_i|C^K) \\ &= \sum_{j=1}^K \sum_{z_i \in [C_{j-1}, C_j)} \log P(z_i|C^K) \\ &= \sum_{j=1}^{K-1} \sum_{z_i \in [C_{j-1}, C_j)} \log P(z_i|\{C^K \setminus C_K\}) + \sum_{z_i \in [C_{K-1}, C_K]} \log P(z_i|C_K) \\ &= \log P(z_{C_{K-1}}^n|\{C^K \setminus C_K\}) + \sum_{z_i \in [C_{K-1}, C_K]} \log P(z_i|C_K) \end{aligned} \quad (19)$$

where $z_{C_K}^n$ is a constrained dataset containing all data points smaller than C_K , i.e.,

$$z_{C_{K-1}}^n = \{z \in z^n \mid z < C_{K-1}\}. \quad (20)$$

Given the previous, the recursion formula is given by

$$\begin{aligned} \max_{C^K \subseteq C_a} \log P(z^n | C^K) &= \max_{C_K \in C_a} \left[\max_{\{C^K \setminus C_K\} \subseteq C_a} \log P(z_{C_{K-1}}^n | \{C^K \setminus C_K\}) \right. \\ &\quad \left. + \sum_{z_i \in [C_{K-1}, C_K]} \log P(z_i | C_K) \right] \end{aligned} \quad (21)$$

and hence a dynamic programming algorithm can be applied, to search all $K \in [K_{max}]$. In practice, K_{max} is pre-determined, and larger K_{max} should be investigated if $\hat{K} = K_{max}$.

The disadvantage of implementing the dynamic programming algorithm based on $L(z^n, C^K)$, $\forall K \in [K_{max}]$, is that we would need to calculate the parametric complexity $\text{COMP}(\cdot)$ for every constrained dataset. Our improved version, in contrast, involves only $P(z^n | C^K)$, and thus we only need to calculate $\text{COMP}(\cdot)$ for the full dataset z^n when calculating $L(z^n, \hat{C}^K)$ for each K , which will be much faster in practice.

The essential component of the dynamic programming algorithm is to construct the constrained dataset $z_{C_{K-1}}^n$, $\forall K \in \{1, \dots, K_{max}\}$. These constrained datasets are easy to construct in the one-dimensional case with a natural order, but infeasible for two or higher dimensional cases.

6 The PALM Algorithm for Partitioning and Merging

We propose a heuristic algorithm named PALM, which infers histogram models for two-dimensional data by decomposing the overall model selection problem into two steps: 1) partition space S alternately based on the discretization result from previous iterations, until it stops automatically; and then 2) merge neighbouring sub-regions if their densities are very similar. Both steps use the MDL principle as criterion, with the code length as defined in Section 4.

We already proved that finding the MDL-optimal cut lines, no matter vertical or horizontal, for a certain sub-region within \tilde{S} , is equivalent to finding the MDL-optimal one-dimensional cut points for the corresponding one-dimensional data, which is the projection of the two-dimensional data on x- or y-axis. The partitioning step of PALM is to iteratively repeat this process until all sub-regions within \tilde{S} stops further partitioning. Note that the direction of the first partitioning could be chosen in a greedy manner, or by the user given the task at hand.

In other words, during the partitioning step, we iteratively consider each subset of the data within each sub-region given by the previous partitioning iteration, in order to capture the local density structures as much as possible. We use the intuition that if the empirical joint probability distribution of (the subset of) data within a sub-region is not approximately uniform, the empirical marginal probability distribution for each individual dimension is probably not uniform either. The only exception is the so-called *copula* (Nelsen, 2007): a copula is a multivariate random variable with its joint probability distribution being non-uniform but all marginal distributions being uniform. However, we assume that such case rarely exists in practice, although it can be easily constructed in theory.

Following the partitioning step, we merge neighbouring regions with similar densities, to refine the histogram model in order to reduce unnecessary boundaries (as well as the number of density estimation parameters), and to better characterise the density structure. The merging step is essentially a model selection problem within a constrained model class, only containing all models that can be obtained by merging neighbouring sub-regions of the partition resulting from the partitioning step. We iteratively examine each neighbouring pair to decide whether we merge or not, until it automatically stops, in a greedy manner.

The full PALM algorithm is described in Algorithm 1.

Algorithm 1 PALM algorithm

Input: data x^n , data precision ϵ , sample space S , maximum number of splits per partitioning step K_{max}

Output: \tilde{S} , a partition of S

- 1: $dir \leftarrow 0$ or 1 ▷ Initial partitioning direction: 0 and 1 represent horizontal and vertical resp.
- 2: **while true do** ▷ Start the partitioning step.
- 3: **for** $S_k \in \tilde{S}$ **do**
- 4: Partition S_k as \tilde{S}_k by finding the optimal cut lines of S_k on direction dir
- 5: $C_{S_k}^* = \arg \min_{C_{S_k}} L(\{x^n \in S_k\}, C_{S_k})$
- 6: **if** $\tilde{S}_k = \{S_k\}$, for all $S_k \in \tilde{S}$ **then**
- 7: **break**
- 8: **else**
- 9: $\tilde{S} \leftarrow \bigcup \tilde{S}_k$
- 10: $dir \leftarrow 1 - dir$
- 11:
- 12: $\tilde{S}_{merge} \leftarrow \tilde{S}$ ▷ Start the merging step.
- 13: $K_{merge} \leftarrow$ the number of sub-regions of \tilde{S}_{merge}
- 14: **while true do**
- 15: Get all neighbouring pairs of sub-regions of \tilde{S}_{merge} , $Pairs \leftarrow \{(S_j, S_k), \dots\}$
- 16: **for** $(S_j, S_k) \in Pairs$ **do**
- 17: $S'_{j,k} \leftarrow$ merge the pair (S_j, S_k) in \tilde{S}_{merge}
- 18: Calculate $L(x^n, \tilde{S}'_{j,k}) = -\log(P(x^n | \tilde{S}'_{j,k})) + \log \text{COMP}(n, K_{merge} - 1)$
- 19: **if** $\min_{S'_{j,k}} L(x^n, \tilde{S}'_{j,k}) > L(x^n, \tilde{S}_{merge})$ **then**
- 20: **return** \tilde{S}_{merge}
- 21: **else**
- 22: $\tilde{S}_{merge} \leftarrow \arg \min_{\tilde{S}'_{i,j}} L(x^n, \tilde{S}'_{i,j})$
- 23: $K_{merge} \leftarrow K_{merge} - 1$

Algorithm complexity. We briefly discuss the algorithm complexity for the partitioning and merging step respectively.

For the first iteration of the partitioning step (i.e., when $\tilde{S} = \{S\}$), the algorithm has a complexity of $\mathcal{O}(K_{max}E^2)$, as in the one-dimensional case (Konkanen and Myllymäki, 2007b), where E is the number of possible locations for vertical (or horizontal) lines within the whole sample space S , based on the fixed grid with granularity ϵ . The second iteration has a worst-case time complexity of $\mathcal{O}(K_{max}^2E^2)$ when the first iteration produces exactly K_{max} sub-regions. Following

this line, the worst-case time complexity of the partitioning step is $\mathcal{O}(K_{max}^I E^2)$, where I is the number of iterations.

As for the merging step, the time complexity is bounded by K_0 , which is the number of sub-regions of the partition after the partitioning step of PALM algorithm.

Although the worst-case time cost for the partitioning step is exponential, and K_0 could be large in practice, we empirically find the whole algorithm to be quite efficient, as will be discussed in Sections 7 and 8.

7 Experiments

In this section, we investigate the performance of PALM using synthetic data, after which we will apply it to real world data in the next section. We show that PALM can construct two-dimensional histograms that are adaptive to both local densities and sample size of the data.

We start off by defining the “loss” that we use for quantifying the quality of the “learned partition” by PALM. We then present experiment results on a wide variety of synthetic data. Although our algorithm relies on heuristics, we show that it has a number of desirable properties nevertheless.

First, if the data is generated by a histogram model within our model class \mathcal{M} , PALM is able to identify that “true” histogram given a large enough sample size. The results are discussed in Section 7.2.

Second, in Section 7.3 we show that PALM has the flexibility to approximate histogram models outside the model class \mathcal{M} . Specifically, we study the behaviour of PALM on a dataset generated as follows: we set the sample size $S = [0, 1] \times [0, 1]$, and partition it by a sine curve; we then generate data points uniformly distributed above and below the sine curve, with different densities.

Third, we study the performance of PALM on data generated by two-dimensional Gaussian distributions, in Section 7.4. We show that it inherits the property of the one-dimensional MDL histogram method (Kontkanen and Myllymäki, 2007b) that the bin size of the histogram is self-adaptive: the two-dimensional bin size becomes smaller locally where the probability density changes more rapidly.

Finally, in Section 7.5 we compare PALM with the IPD algorithm (Nguyen et al., 2014), using a simple synthetic dataset that is almost the same as what has been used to study the performance of the IPD algorithm (Nguyen et al., 2014).

Note that we always set $\epsilon = 0.001$, and all simulations are repeated 500 times, unless specified otherwise. The initial partitioning direction is fixed as vertical, to make the visualisations of the inferred partitions comparable.

7.1 Measuring the difference between two-dimensional histograms

Now we discuss how we measure the quality of the learned partition by PALM. As PALM produces a histogram model and can be regarded as a density estimation method, one of the most intuitive “loss” functions is the *Mean Integrated Squared Error (MISE)* (Scott, 2015), defined as

$$\text{MISE}(\hat{f}) = \mathbb{E}\left[\int_S (f(x) - \hat{f}(x))^2 dx\right], \quad (22)$$

where f is the true probability density and \hat{f} is the histogram model density estimator. We report the empirical MISE by calculating the integral numerically, and estimating $\mathbb{E}[\cdot]$ by the empirical mean of results over all repetitions of the simulation.

As MISE cannot indicate whether there are more “bins” than necessary, we also propose two “loss” functions that directly quantify the distances between the inner boundaries of the learned and true partitions of a sample space S . We first break up the line segments of the inner boundaries into *pixels* with a precision set to $0.01 = 10\epsilon$ (merely to speed up the calculation). Then we introduce two loss functions using the idea of *Hausdorff distance*, but consider *false positive* and *false negative* respectively. Namely, we propose L_{learn} , based on the learned partition, and L_{true} , based on the true partition:

$$L_{\text{learn}} = \sum_{p \in P} \min_{q \in Q} \|p - q\|^2; L_{\text{true}} = \sum_{q \in Q} \min_{p \in P} \|p - q\|^2 \quad (23)$$

where $\|\cdot\|$ denotes the Euclidean distance and P and Q are the sets of *pixels* on line segments of the learned partition and the true partition, respectively.

To interpret these two “loss” functions: if L_{learn} is large, the learned partition must have unnecessary extra line segments, whereas if L_{true} is large, the learned partition fails to identify part of the line segments that actually exist.

7.2 Revealing the ground truth two-dimensional histogram

We describe the settings for simulating the data and then our experiment results, to empirically show that our algorithm can identify the “true” histogram model if the data is generated by it.

Experiment settings. To randomly generate the “true” partitions, we use a generative process that is very similar to the search process of our algorithm: we fix a rectangular region, $S = [0, 1] \times [0, 1]$, randomly generate vertical cut lines to split it into K_1 sub-regions, and randomly generate horizontal cut lines to split each of the K_1 regions into $(K_{21}, \dots, K_{2, K_1})$ sub-regions respectively. Then, for each pair of neighbouring sub-regions, we merge them with a pre-determined probability P_{merge} .

We set these hyper parameters as follows:

$$K_1 = K_{21} = K_{22} = \dots = K_{2, K_1} = 5; P_{\text{merge}} = 0.4; \epsilon = 0.001. \quad (24)$$

With these hyper parameters, our generative process is able to generate a diverse subset of \mathbb{M} , as P_{merge} is chosen delicately to be not too small or too large. Figure 2 shows four random examples of how the true partitions and learned partitions look like. These learned partitions are produced when the sample size is set as 10 000.

After the partition is fixed, we also generate “true” density parameters for the histogram model, f_j , using a uniform distribution, i.e.,

$$f_j \sim \text{Uniform}(0, 1), \forall i = 1, 2, \dots, K; \quad (25)$$

and normalise them such that $\sum_{j=1}^K f_j |S_j| = 1$, where K is the number of sub-regions in total and $|S_j|$ is the geometric area of S_j . Note that we do not force the f_j to be different from each other.

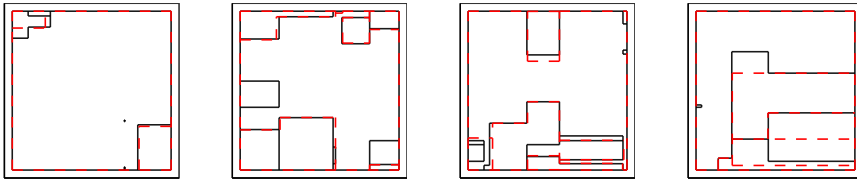


Fig. 2 Random examples of true (black solid) and learned partitions (red dashed) of the experiment in Section 7.2, mainly to show that our experiment settings can produce very flexible partitions of $[0, 1] \times [0, 1]$. Note that the sample size is set as 10000, which is *not* enough for MISE (Equation 22) to converge to almost 0, but the learned partitions by PALM already look promising: it can partly identify the true partitions.

Results. Figure 3 shows that MISE converges to almost 0 as the sample size increases. We also show, in Figure 4, that L_{learn} and L_{true} converge to almost zero except for some outliers.

The outliers of L_{learn} are due to sampling variance when generating data points, the number of which decreases significantly as the sample size grows.

The outliers of L_{true} , however, are due to the random generation of the density parameters f_j . As we do not force all f_j 's to be different at least to a certain degree, they could accidentally turn out to be very similar. In that case, some of the “true” inner boundaries are actually unnecessary, and our algorithm will “fail” to discover them. Table 1 confirms that this is the cause of those outliers when the sample size is large ($\geq 1e5$): when PALM fails to identify part of the “true” inner boundaries and $L_{\text{true}} > 1$, the learned histogram still estimates the density very accurately. The only explanation is then that some sub-regions of the true partition accidentally have very similar f_j 's and PALM “fails” to partition them.

Moreover, when the sample size is moderate, e.g., 5000, L_{learn} is already small, meaning that PALM can partly identify the true partition quite precisely, and rarely produce unnecessary extra sub-regions. As the sample size increases, L_{true} decreases, indicating that the learned partition becomes more and more complex; i.e., it is shown that the model selection process is self-adaptive to sample size.

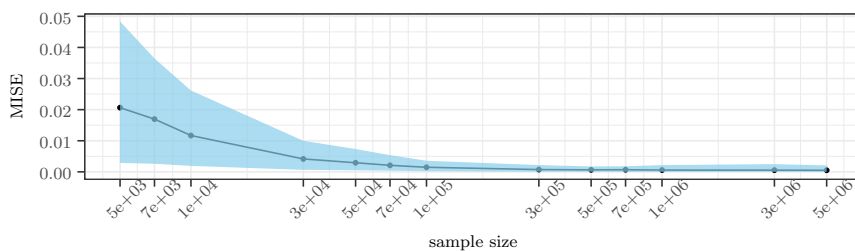


Fig. 3 Sample size vs MISE: MISE converges to almost 0 when sample size becomes larger 100000. The range between the 5th and 95th percentiles is shown in blue.

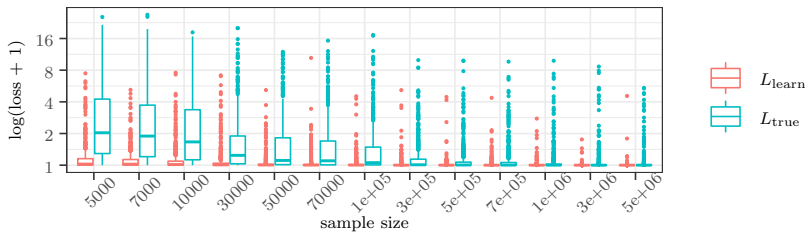


Fig. 4 Sample size versus L_{learn} and L_{true} as defined in Equation (23). Note that the y-axis has a logarithmic scale. L_{learn} is generally much smaller than L_{true} , meaning that it is very rare that PALM produces unnecessary extra sub-regions. When the sample size is large enough for MISE to converge ($n \geq 1e5$), outliers of L_{true} are due to sampling variance when generating the true parameters f_j defined in Equation (25), see Table 1; the number of outliers for L_{learn} decreases rapidly as the sample size becomes larger, as they are due to sampling variance when generating the data.

Sample size	MISE for subgroup: $L_{\text{true}} > 1$	overall MISE
100 000	0.00148	0.00148
300 000	0.00055	0.00074
500 000	0.00051	0.00065
700 000	0.00019	0.00069
1 000 000	0.00023	0.00058
3 000 000	0.00017	0.00055
5 000 000	0.00006	0.00051

Table 1 The average MISE of cases when $L_{\text{true}} > 1$, and the overall mean of MISE. We show that, when PALM fails to identify part of the true partitions, the learned histogram model still estimates the probability density accurately. The only explanation for these cases is that some neighbouring sub-regions in the true partitions have very similar “true” f_j as defined in Equation (25), and PALM fails to identify line segments that partition these neighbouring sub-regions.

7.3 Approximations histogram models outside model class \mathbb{M}

We now investigate the case where the true model is not within model class \mathbb{M} , while the data is still generated uniformly within each sub-region.

We show that, although the model class \mathbb{M} is based on a grid, it is indeed very flexible and expressive: in practice, the learned partitions can approximate true partitions outside \mathbb{M} , and the approximation becomes more and more accurate as the sample size grows.

Experiment settings. As an illustrative example, we partition $S = [0, 1] \times [0, 1]$ by several sine curves, defined as

$$g(x) = \frac{1}{4} \sin 2m\pi x + \frac{1}{2} \quad (26)$$

and where m is a hyper-parameter.

We randomly generate data from a uniform distribution above and under the sine curve, and we set the probability density above $g(x)$ to be twice as large as below $g(x)$, i.e., we uniformly sample $\frac{2}{3}n$ data points above $g(x)$, and $\frac{1}{3}n$ data points below $g(x)$, where n is the total sample size.

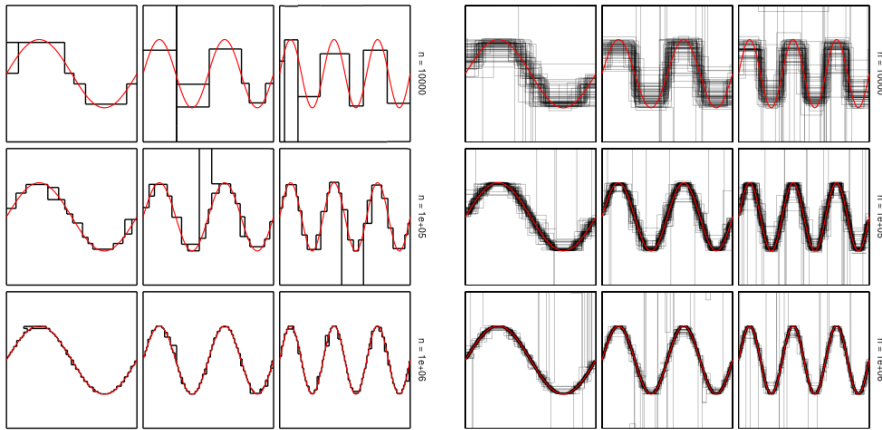


Fig. 5 (Left) Sine curve defined in Equation (26) (red), with $m \in \{2, 4, 6\}$ from left to right on each row, and the learned partition by PALM (black). Data is randomly generated by uniform distribution above and below the sine curve, within $S = [0, 1] \times [0, 1]$. Densities above and below the sine curve are 2:1. From top to bottom, the sample sizes of the simulated data is $n \in \{1e4, 1e5, 1e6\}$. (Right) 50 partition results of 50 different simulated datasets are plotted together. It shows that PALM is not guaranteed to be absolutely stable, as it occasionally produces undesired extra line segments, but the line segments of learned partitions mostly gather around the true sine curve.

Results. We empirically show that the learned partitions approximate the sine curves quite precisely, though occasionally a few extra undesired sub-regions are produced. Figure 5 (left) shows the learned partitions on single simulated datasets, with $m \in \{2, 4, 6\}$ to control the degree of oscillation, and sample size $n \in \{1e4, 1e5, 1e6\}$. We see that, as the sample size grows, our approximation becomes more and more accurate.

However, since our algorithm is greedy in nature, there is no guarantee to find the partition with the global minimum score. As for this case, PALM will occasionally produce undesired, extra line segments. Thus, to investigate the stability of the learned partitions, we repeat the simulation 50 times for each combination of m and n , and plot *all* partition results in one single plot in Figure 5 (right).

Figure 5 (right) shows that the undesired extra sub-regions are produced more frequently as m increases, but seems independent of sample size n . However, as sample size increases, the learned partitions become indeed more stable as they gather around the sine curves more closely.

7.4 Gaussian random variables

In this section, we show the performance of our algorithm on data generated by two-dimensional Gaussian distribution. Specifically, we consider two of them, i.e., $N\left[\begin{pmatrix} 0 \\ 0 \end{pmatrix}, \begin{pmatrix} 1 & 0 \\ 0 & 1 \end{pmatrix}\right]$ and $N\left[\begin{pmatrix} 0 \\ 0 \end{pmatrix}, \begin{pmatrix} 1 & 0.5 \\ 0.5 & 1 \end{pmatrix}\right]$, of which the key difference is whether the two dimensions are independent. We assume $S = [-5, 5] \times [-5, 5]$, as the true Gaussian density outside such S is negligible.

Figure 7 shows the learned partitions as well as the learned empirical densities from a random simulated dataset with different sample sizes $n \in \{5\,000, 10\,000\}$,

50 000}. Note that the bin size is self-adaptive with regard to sample size and local structure of the probability density. We also mention that the empirical runtime for a single dataset generated by such Gaussian distributions is at most a few minutes, for all $n \leq 50\,000$.

To quantify the quality of the learned partitions by PALM, we compare the MISE of PALM to the MISE of fixed equally-spaced grid partitions with different granularities. Figure 6 shows the mean and standard deviation of MISE for different cases, and we conclude that, to achieve roughly the same level of MISE with a fixed grid, the fixed grid needs to have five times as many sub-regions as the learned partition by PALM.

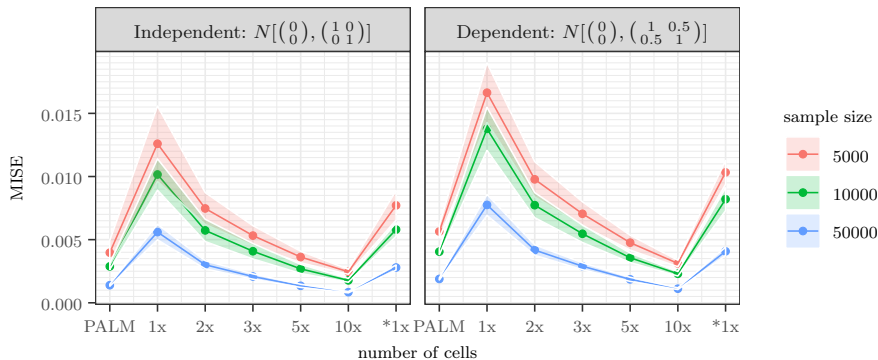


Fig. 6 For data generated from a two-dimensional Gaussian distribution, described in Section 7.4, the mean and standard deviation of MISE is calculated for different partitions: (from left to right) PALM, fixed grid with the same number of sub-regions as PALM (denoted as ‘1x’), fixed grid with two times number of sub-regions as PALM (denoted as ‘2x’), ..., and fixed grid with the same number of sub-regions before the merging step of PALM (denoted as ‘*1x’). We assume $S = [-5, 5] \times [-5, 5]$, as the true Gaussian density outside S is negligible.

7.5 Comparison with IPD

Since—to the best of our knowledge—no existing discretization method can produce partitions as expressive as PALM, it seems not so meaningful to compare with any existing algorithm. However, we do include a comparison with the IPD algorithm (Nguyen et al., 2014), mainly to show that our algorithm not only can produce more flexible partitions by definition, but also beats this state-of-the-art algorithm on a “simple” task, i.e., when the “true” partition is an adaptive two-dimensional grid.

We use simple synthetic data, the same as what has been used to study the performance of the IPD algorithm (Nguyen et al., 2014). The data is generated to be uniform within four sub-regions within $S = [0, 1] \times [0, 1]$. These sub-regions are produced by partitioning S by one vertical line $x = V_x$ and one horizontal line $y = H_y$, where $V_x, H_y \sim \text{Uniform}(0, 1)$. The number of data points within each sub-region are equal.

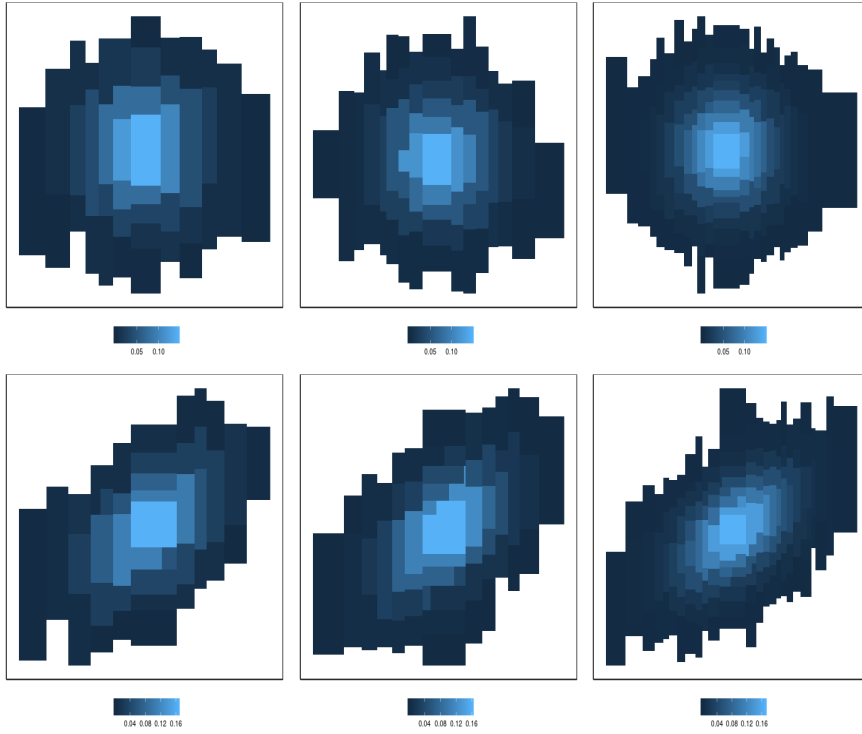


Fig. 7 Learned partitions and estimated densities by PALM. The data is generated from two-dimensional Gaussian distributions, with sample size $n \in \{5\,000, 10\,000, 50\,000\}$, from left to right. The top and bottom row is respectively generated from independent and dependent two-dimensional Gaussian distributions.

We compare the loss, as defined in Equation (23), and we show that 1) PALM has better performance on small datasets, and 2) as the sample size gets larger, PALM converges but IPD partitions S into more and more sub-regions, as can be witnessed from an increasing L_{true} (Figure 8).

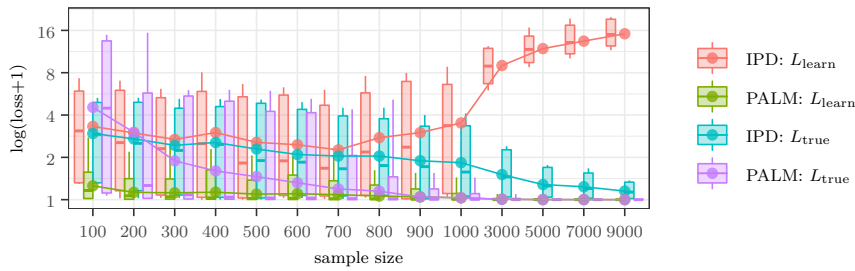


Fig. 8 Comparison of PALM and IPD, using box-plot and mean L_{learn} and L_{true} defined in Equation (23). PALM not only performs better when sample size is small, but also converges as sample size grows, while IPD does not converge.

8 Case study

We now show the results of applying our algorithm to real world data. We consider two real world datasets: 1) a dataset of GPS locations of Airbnb housing in Amsterdam, and 2) a dataset of GPS locations of destinations of taxi queries of DiDi (a Chinese taxi Mobile App) in Chengdu, China. We thank InsideAirbnb¹ and DiDi² for providing the data.

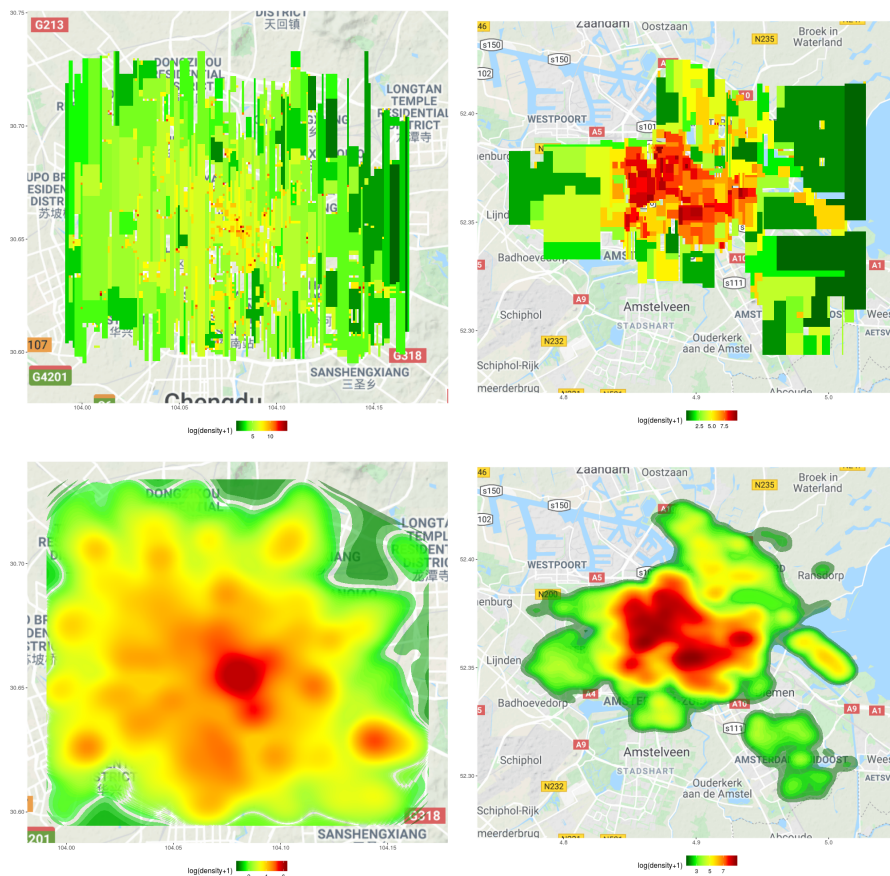


Fig. 9 (Top) Partitions and corresponding empirical densities learned by PALM on real world data: GPS locations of destinations of queries for taxi in Chengdu CHINA using the Mobile App DiDi (upper-left), and GPS locations of Airbnb housing supplies in Amsterdam (upper-right). (Bottom) Kernel density estimation (KDE) on destinations of taxi queries (lower-left) and housing locations (lower-right).

DiDi taxi data in Chengdu. The sample size of the data is 14219. The precision of the dataset is set as $\epsilon = 0.001$, which is roughly 100 meters, even though it was

¹ <http://insideairbnb.com>

² <https://gaia.didichuxing.com>

recorded slightly more precisely. During the partitioning step, we set $K_{max} = 300$ to make sure that $\hat{K} < K_{max}$. We also assume S to be the smallest rectangle that covers all the data points. The initial partitioning direction is set as vertical.

The empirical runtime for this dataset is about 36 minutes on a personal desktop computer.

Figure 9 (left) shows the partition and density estimation results by PALM (top left) and by kernel density estimation (bottom left). Specifically, for the kernel density estimation (KDE), Gaussian kernel is used and the bandwidth is chosen by Silverman’s ‘rule of thumb’ (Sheather, 2004). When plotting the KDE results, the number of contours is forced to partition S into the same number of sub-regions as PALM does for each dataset.

While KDE only reveals the density structure on a high level, PALM is able to accurately detect dense “spots”, which is more realistic as the most popular regions of taxi destinations in a big city (e.g., shopping malls, restaurant & bar streets, central business district) are not expected to be much bigger than ϵ^2 (i.e., 100 meters \times 100 meters).

Amsterdam Airbnb housing locations. This data has a sample size of 20 244. As above, the precision is set as $\epsilon = 0.001$, $K_{max} = 300$, and the initial partitioning direction is vertical.

Figure 9 (right) shows the partition and density estimation results by PALM (top right) and by KDE (bottom right), with the same settings for hyper parameters and for plotting as above. We can see that although the general density structures revealed by PALM and KDE are similar, PALM provides much more informative local density structure in the dense regions.

Note that although the sample sizes for both datasets are comparable, the density structures revealed by PALM are totally different, showing that PALM not only is self-adaptive to the sample size, but also self-adaptive to local density structures that occur in the data.

9 Conclusions

We propose a novel two-dimensional discretisation method based on the MDL principle. By dividing the model selection task into a partitioning step and a merging step, we simultaneously solve two problems: one is to encode the histogram model and calculate the corresponding code length in a “proper” way; the other is to provide a search strategy not only intuitive and interpretable, but also performs well in practice, both on synthetic and real-world datasets.

We next mention the applicability of the PALM algorithm to higher dimensions. Firstly, the idea of dividing the model selection task into the partitioning and merging step can be directly used for higher dimensions. The corresponding code length of data would only differ by a constant as we proved, while the code length of model may include another term, which is the code length needed to encode which dimension to be split further. Therefore, conceptually it seems trivial to extend PALM to higher dimensions, although the method may suffer from the curse of dimensionality and high computational cost. We leave the exploration and investigation as future work.

References

- Bay SD (2001) Multivariate discretization for set mining. *Knowledge and Information Systems* 3(4):491–512
- Biba M, Esposito F, Ferilli S, Di Mauro N, Basile TMA (2007) Unsupervised discretization using kernel density estimation. In: *IJCAI*, pp 696–701
- Breiman L (2017) *Classification and regression trees*. Routledge
- Cuevas A, Fraiman R, et al. (1997) A plug-in approach to support estimation. *The Annals of Statistics* 25(6):2300–2312
- Fayyad U, Irani K (1993) Multi-interval discretization of continuous-valued attributes for classification learning
- Ferrandiz S, Boullé M (2005) Multivariate discretization by recursive supervised bipartition of graph. In: *International Workshop on Machine Learning and Data Mining in Pattern Recognition*, Springer, pp 253–264
- Friedman J, Hastie T, Tibshirani R (2001) *The elements of statistical learning*, vol 1. Springer series in statistics New York
- Grünwald P, Roos T (2019) Minimum description length revisited. arXiv preprint arXiv:190808484
- Grünwald PD (2007) *The minimum description length principle*. MIT press
- Gupta A, Mehrotra KG, Mohan C (2010) A clustering-based discretization for supervised learning. *Statistics & probability letters* 80(9-10):816–824
- Han J, Cheng H, Xin D, Yan X (2007) Frequent pattern mining: current status and future directions. *Data mining and knowledge discovery* 15(1):55–86
- Hansen MH, Yu B (2001) Model selection and the principle of minimum description length. *Journal of the American Statistical Association* 96(454):746–774
- Jörnsten R, Yu B (2003) Simultaneous gene clustering and subset selection for sample classification via mdl. *Bioinformatics* 19(9):1100–1109
- Kameya Y (2011) Time series discretization via mdl-based histogram density estimation. In: *2011 IEEE 23rd International Conference on Tools with Artificial Intelligence*, IEEE, pp 732–739
- Kang Y, Wang S, Liu X, Lai H, Wang H, Miao B (2006) An ica-based multivariate discretization algorithm. In: *International Conference on Knowledge Science, Engineering and Management*, Springer, pp 556–562
- Kontkanen P, Myllymäki P (2007a) A linear-time algorithm for computing the multinomial stochastic complexity. *Information Processing Letters* 103(6):227–233
- Kontkanen P, Myllymäki P (2007b) Mdl histogram density estimation. In: *Artificial Intelligence and Statistics*, pp 219–226
- Kotsiantis S, Kanellopoulos D (2006) Discretization techniques: A recent survey. *GESTS International Transactions on Computer Science and Engineering* 32(1):47–58
- Leibe B, Leonardis A, Schiele B (2008) Robust object detection with interleaved categorization and segmentation. *International journal of computer vision* 77(1-3):259–289
- Liu L, Wong WH (2014) Multivariate density estimation based on adaptive partitioning: Convergence rate, variable selection and spatial adaptation. arXiv preprint arXiv:14012597
- Luo Q, Khoshgoftaar TM (2006) Unsupervised multiscale color image segmentation based on mdl principle. *IEEE Transactions on Image Processing* 15(9):2755–

2761

- Mehta S, Parthasarathy S, Yang H (2005) Toward unsupervised correlation preserving discretization. *IEEE Transactions on Knowledge and Data Engineering* 17(9):1174–1185
- Nelsen RB (2007) An introduction to copulas. Springer Science & Business Media
- Nguyen HV, Müller E, Vreeken J, Böhm K (2014) Unsupervised interaction-preserving discretization of multivariate data. *Data Mining and Knowledge Discovery* 28(5-6):1366–1397
- Niblack TKDW, Steele D (1994) A fast algorithm for mdl-based multi-band image segmentation. In: *Proc. IEEE Computer Vision and Pattern Recognition Conf*, pp 609–616
- Pfahring B (1995) Compression-based discretization of continuous attributes. In: *Machine Learning Proceedings 1995*, Elsevier, pp 456–463
- Ram P, Gray AG (2011) Density estimation trees. In: *Proceedings of the 17th ACM SIGKDD international conference on Knowledge discovery and data mining*, pp 627–635
- Rissanen J (1978) Modeling by shortest data description. *Automatica* 14(5):465–471
- Robnik-Šikonja M, Kononenko I (1998) Pruning regression trees with mdl. In: *Proceedings of the 13th European Conference on Artificial Intelligence*, John Wiley & Sons, Chichester, England, pp 455–459
- Scott DW (2015) *Multivariate density estimation: theory, practice, and visualization*. John Wiley & Sons
- Sheather SJ (2004) Density estimation. *Statistical science* pp 588–597
- Vreeken J, Van Leeuwen M, Siebes A (2011) Krimp: mining itemsets that compress. *Data Mining and Knowledge Discovery* 23(1):169–214
- Yang K, Wong WH (2014) Density estimation via adaptive partition and discrepancy control. arXiv preprint arXiv:14041425
- Zhang XH, Wu J, Lu TJ, Jiang Y (2007) A discretization algorithm based on gini criterion. In: *2007 International Conference on Machine Learning and Cybernetics, IEEE*, vol 5, pp 2557–2561

10 Appendix A: Proof that $\text{COMP}(n, \tilde{S})$ is independent of the number of dimensions (Section 4.1)

Assume $S \subset \mathbb{R}^l$, \tilde{S} is any partition of S with K sub-regions, and $\forall S_j \in \tilde{S}$, $|S_j|$ represents the (hyper-)volume of S_j ; for any y^n that can be generated by \tilde{S} , $h_j(y^n)$ denotes the number of data points in sub-region S_j .

$$\begin{aligned}
\text{COMP}(n, \tilde{S}) &= \sum_{y^n \in S^n} P(y^n | \tilde{S}_{\mathbf{f}=\hat{\mathbf{f}}(y^n)}) \\
&= \sum_{y^n \in S^n} \left[\prod_{j=1}^K \left(\frac{h_j(y^n) \epsilon^l}{n |S_j|} \right)^{h_j} \right] \\
&= \sum_{h_1 + \dots + h_K = n, h_j \geq 0, \forall j} \sum_{\{y^n : h_j(y^n) = h_j, \forall j\}} \left[\prod_{j=1}^K \left(\frac{h_j(y^n) \epsilon^l}{n |S_j|} \right)^{h_j} \right]
\end{aligned} \tag{27}$$

To count the elements in the set $\{y^n : h_j(y^n) = h_j, \forall j\}$, we observe that the number of possible ways of distributing (h_1, \dots, h_K) data points into each sub-region of \tilde{S} respectively is

$$\binom{n}{h_1} \binom{n-h_1}{h_2} \dots \binom{n-h_1-\dots-h_{K-1}}{h_K} = \frac{n!}{h_1! \dots h_K!}. \tag{28}$$

As we assume the precision to be ϵ , for any S_j , the number of possible locations for those $h_j(y^n)$ points is equal to $\left(\frac{|S_j|}{\epsilon^l}\right)^{h_j}$. Thus, the number of elements in the set $\{y^n : h_j(y^n) = h_j, \forall j\}$ is

$$\frac{n!}{h_1! \dots h_K!} \prod_{j=1}^K \left(\frac{|S_j|}{\epsilon^l} \right)^{h_j} \tag{29}$$

Therefore,

$$\begin{aligned}
\text{COMP}(n, \tilde{S}) &= \sum_{h_1 + \dots + h_K = n} \left[\frac{n!}{h_1! \dots h_K!} \prod_{j=1}^K \left(\frac{|S_j|}{\epsilon^l} \right)^{h_j} \prod_{j=1}^K \left(\frac{h_j \cdot \epsilon^l}{n \cdot |S_j|} \right)^{h_j} \right] \\
&= \sum_{h_1 + \dots + h_K = n} \left[\frac{n!}{h_1! \dots h_K!} \prod_{j=1}^K \left(\frac{|S_j|}{\epsilon^l} \right)^{h_j} \left(\frac{h_j \cdot \epsilon^l}{n \cdot |S_j|} \right)^{h_j} \right] \\
&= \sum_{h_1 + \dots + h_K = n} \frac{n!}{h_1! \dots h_K!} \prod_{j=1}^K \left(\frac{h_j}{n} \right)^{h_j},
\end{aligned} \tag{30}$$

which completes the proof.

Note that for continuous data y^n , $\text{COMP}(n, \tilde{S})$ becomes an integral over $y^n \in S^n$, but by the definition of Riemann integral, (which always exists since ϵ cancels out), the result of $\text{COMP}(n, \tilde{S})$ is the same as Equation (30).

11 Appendix B: Proof that only searching for cut points that are closest to data points is sufficient (Section 6)

Consider one-dimensional data z^n , and a partition of the data space S , by a set of cut points, denoted as $C^K = \{C_0 = \min z^n, C_1, \dots, C_K = \max z^n\}$, the probability of data is

$$P(z^n|C^K) = \prod_{j=1}^K \left(\frac{h_j \epsilon}{n|S_j|} \right)^{h_j} \quad (31)$$

where h_j is the number of data points within the subinterval S_j , and $|S_j|$ is the length of the subinterval S_j .

We regard $P(x^n|C^K)$ as a *continuous* function of the vector $\mathbf{S} = (|S_1|, \dots, |S_K|)$, i.e., we forget about the granularity ϵ for now, and clearly all h_j 's are fixed once we fix the \mathbf{S} .

On the other hand, if we keep all h_j 's fixed, we can still "move" all the cut points to change \mathbf{S} while keeping the h_j 's fixed, i.e., we can move a cut point $x = V_x$ within some closed interval, denoted as $[a, b]$, within which no data points exist.

We prove that the maximum of $P(x^n|C^K)$ will always be achieved when $V_x = a$ or $V_x = b$ as we keep other cut points fixed. By doing this, we also prove that, given candidate cut points, we only need to consider cut points that are near to the data points, i.e., if for any candidate cut point, it is another two cut points that are closest to it, other than one or more data points, we can then skip this candidate cut point.

Since when we move one single cut point, it only affects the subinterval left and right to that cut point, while all other $|S_j|$'s remain the same, it is sufficient to just prove for the case $K = 2$.

Since now $C_0 = \min_{i \in [n]} x_{i1}$ and $C_2 = \max_{i \in [n]} x_{i1}$, $P(x^n|C^2)$ becomes a function of C_1 , and equivalently a function of $|S_1|$, where both C_1 and $|S_1|$ are bounded as we need to keep h_1 and h_2 fixed, i.e.,

$$\log P(x^n|C^2) = \log \left(\left(\frac{\epsilon h_1}{n|S_1|} \right)^{h_1} \left(\frac{\epsilon h_2}{n(|S| - |S_1|)} \right)^{h_2} \right) \quad (32)$$

where we assume $|S_1| \in [a, b]$ for some certain closed interval $[a, b]$. As we want to maximize $\log P(x^n|C^2)$, it is equivalent to *minimizing*

$$F(|S_1|) := h_1 \log |S_1| + h_2 \log (|S| - |S_1|) \quad (33)$$

as other terms in Equation (32) are constant. Since

$$F'(|S_1|) = \frac{h_1(|S| - |S_1|) - h_2|S_1|}{(|S| - |S_1|)|S_1|}, \quad (34)$$

by setting $F'(|S_1|) = 0$, we have

$$|S_1|^* = \frac{h_1}{h_1 + h_2} L \quad (35)$$

We also check

$$F''(|S_1|) = \frac{-(h_1 + h_2)|S_1|^2 + 2h_1|S||S_1| - h_1|S|^2}{(|S| - |S_1|)^2|S_1|^2} < 0 \quad (36)$$

because,

$$(2h_1|S|)^2 - 4(-(h_1 + h_2))(h_1|S|^2) = -4h_2h_1|S_1|^2 < 0 \quad (37)$$

as $h_1, h_2, |S_1| > 0$. Therefore, if $|S_1|^* \notin [a, b]$, $F(|S_1|)$ is monotonic within $[a, b]$; if $|S_1|^* \in [a, b]$, $|S_1|^*$ reaches the maximum. In both cases, the minimum of $F(|S_1|)$ will be either a or b , which completes the proof.